

Observing the Inflationary Reheating

Jérôme Martin,^{1,*} Christophe Ringeval,^{2,†} and Vincent Vennin^{3,‡}

¹*Institut d'Astrophysique de Paris, UMR 7095-CNRS,
Université Pierre et Marie Curie, 98 bis boulevard Arago, 75014 Paris, France*

²*Centre for Cosmology, Particle Physics and Phenomenology,
Institute of Mathematics and Physics, Louvain University,
2 Chemin du Cyclotron, 1348 Louvain-la-Neuve, Belgium*

³*Institute of Cosmology & Gravitation, University of Portsmouth,
Dennis Sciama Building, Burnaby Road, Portsmouth, PO1 3FX, United Kingdom*

(Dated: September 5, 2018)

Reheating is the the epoch which connects inflation to the subsequent hot Big-Bang phase. Conceptually very important, this era is, however, observationally poorly known. We show that the current Planck satellite measurements of the Cosmic Microwave Background (CMB) anisotropies constrain the kinematic properties of the reheating era for most of the inflationary models. This result is obtained by deriving the marginalized posterior distributions of the reheating parameter for about 200 models taken in *Encyclopædia Inflationaris*. Weighted by the statistical evidence of each model to explain the data, we show that the Planck 2013 measurements induce an average reduction of the posterior-to-prior volume by 40%. Making some additional assumptions on reheating, such as specifying a mean equation of state parameter, or focusing the analysis on peculiar scenarios, can enhance or reduce this constraint. Our study also indicates that the Bayesian evidence of a model can substantially be affected by the reheating properties. The precision of the current CMB data is therefore such that estimating the observational performance of a model now requires incorporating information about its reheating history.

PACS numbers: 98.80.Cq

The recent release of high accuracy Cosmic Microwave Background (CMB) data by the Planck satellite [1] has made it possible to drastically improve our knowledge of inflation, in particular the slow-roll phase during which the expansion of the early Universe is accelerated [2, 3]. But how inflation ends remains observationally poorly known. The so-called reheating era [4–13] is conceptually of major significance for several reasons. Reheating explains how inflation is connected to the subsequent hot Big-Bang phase and drives the production of all types of matter at its onset. Because the micro-physics of reheating depends on the interaction between the inflaton and the other fundamental fields, by constraining this era, one can learn about these couplings. Furthermore, reheating is sensitive to the shape of the inflationary potential in a field regime that is different from where slow-roll inflation takes place. Finally, once the inflaton decay products have thermalized, the radiation dominated era starts and, for the first time in its history, the Universe as a whole acquires a temperature. Measuring this “reheating temperature” is of crucial importance to understanding the thermal history of the Universe.

For all these reasons, any experimental constraint on the reheating era is highly desirable. In the present letter, we make use of the method developed in Refs. [14–19] (see also Refs. [20, 21]) and show that the Planck 2013 CMB data put non-trivial constraints on the reheating era for essentially all the slow-roll single-field models, which are the scenarios preferred by the data [3, 22, 23].

Constraints on the reheating stage from CMB data

have been first discussed in Refs. [14, 17] using the WMAP three- and seven-year measurements [24, 25]. It was shown that, for the small and large-field inflationary models, reheating histories exhibiting a negative equation of state parameter were constrained to have a reheating temperature higher than the TeV energy scale. Since then the situation has significantly improved, notably thanks to the Planck 2013 data release [1] but also to our ability to derive reheating-consistent observational predictions for a much wider survey of inflationary scenarios [3, 22].

In the following, we make use of the Planck 2013 data to derive the posterior probabilities of the reheating parameters associated with almost 200 inflationary models taken from the *Encyclopædia Inflationaris* [3]. Such a number is representative of all the single-field slow-roll models with canonical kinetic term that have been proposed so far and enables us to extract new constraints and to draw generic conclusions on the inflationary reheating within slow roll. So far, results were known only for very peculiar reheating histories and/or priors [2] and, therefore, our work represents the first general study of how Planck 2013 can constrain the end of inflation.

Let us now see how the reheating phase affects inflationary observables. Within a given inflationary model, and for fixed values of the parameters characterizing the shape of the potential, cosmic inflation stops at a well-determined energy density ρ_{end} . The redshift z_{end} at which this occurs is of crucial importance as it relates the physical value of any length scale measured today to

those during inflation. Denoting by the index “reh” the end of the reheating era, straightforward manipulations yield

$$\begin{aligned} 1 + z_{\text{end}} &= \frac{a_{\text{reh}}}{a_{\text{end}}} (1 + z_{\text{reh}}) = \frac{a_{\text{reh}}}{a_{\text{end}}} \left(\frac{\rho_{\text{reh}}}{\tilde{\rho}_\gamma} \right)^{1/4} \\ &= \frac{a_{\text{reh}}}{a_{\text{end}}} \frac{\rho_{\text{reh}}^{1/4} \rho_{\text{end}}^{1/4}}{\rho_{\text{end}}^{1/4} \tilde{\rho}_\gamma^{1/4}} \equiv \frac{1}{R_{\text{rad}}} \left(\frac{\rho_{\text{end}}}{\tilde{\rho}_\gamma} \right)^{1/4}, \end{aligned} \quad (1)$$

where a is the Friedmann-Lemaître-Robertson-Walker scale factor. The quantity $\tilde{\rho}_\gamma$ stands for the energy density of radiation today rescaled by the number of relativistic degrees of freedom. Such an expression shows that, even within a completely specified inflationary scenario, z_{end} and thus all inflationary observables, are affected by z_{reh} . The last line of Eq. (1) should be understood as a definition of the reheating parameter R_{rad} . It equals unity either for instantaneous reheating ($\rho_{\text{reh}} = \rho_{\text{end}}$) or if reheating is radiation dominated. As shown in Ref. [17], the reheating parameter also verifies

$$\ln R_{\text{rad}} = \frac{\Delta N}{4} (3\bar{w}_{\text{reh}} - 1) = \frac{1 - 3\bar{w}_{\text{reh}}}{12(1 + \bar{w}_{\text{reh}})} \ln \left(\frac{\rho_{\text{reh}}}{\rho_{\text{end}}} \right), \quad (2)$$

where $\Delta N \equiv N_{\text{reh}} - N_{\text{end}}$ is the duration of reheating in e-folds ($N = \ln a$) and \bar{w}_{reh} is the mean value of the equation of state parameter defined by

$$\bar{w}_{\text{reh}} \equiv \frac{1}{\Delta N} \int_{N_{\text{end}}}^{N_{\text{reh}}} \frac{P(n)}{\rho(n)} dn, \quad (3)$$

where P is the total pressure. All these expressions are fully generic and do not assume anything about the microphysics of the reheating process. In addition, as shown in Refs. [26–28], the above parametrization is the most generic as it remains valid even in presence of any additional entropy production eras that could occur after reheating.

Let us now explain how constraints on reheating can be inferred. Each inflationary model \mathcal{M}_i is characterized by some parameters θ_{inf} , describing the slow-roll phase, and θ_{reh} , describing the reheating phase. A complete cosmological scenario also includes the post-inflationary history, characterized by the cosmological parameters θ_{cos} . Here the θ_{cos} have been chosen to be those of a flat Λ CDM Universe complemented by the astrophysical and experimental nuisance parameters associated with the Planck satellite [1]. The inflationary models considered in our analysis are listed in Ref. [3] in which the number and physical meaning of the θ_{inf} are detailed. As mentioned above, the most generic parametrization of reheating is given by only one parameter R_{rad} . However, from a data analysis point of view, it is more convenient to consider $\theta_{\text{reh}} = R_{\text{reh}}$ where

$$R_{\text{reh}} \equiv R_{\text{rad}} \frac{\rho_{\text{end}}^{1/4}}{M_{\text{Pl}}} \quad (4)$$

is a rescaled reheating parameter [14, 26]. Within each \mathcal{M}_i , the energy at the end of inflation is completely specified and both parameters, R_{rad} and R_{reh} , are in one-to-one correspondence. The advantage of R_{reh} over R_{rad} is that it minimizes degeneracies in parameter space. Starting from some motivated prior probability distributions for each \mathcal{M}_i , the Planck CMB data, D , can be used to derive the posterior probability distributions in the parameter space $\{\theta_{\text{inf}}, \theta_{\text{reh}}, \theta_{\text{cos}}\}$. By marginalization over the θ_{inf} and θ_{cos} , one finally obtains the marginalized posterior $\mathcal{P}(\theta_{\text{reh}}|D, \mathcal{M}_i)$ we are interested in [29, 30]. If this posterior is “more peaked” than the prior $\pi(\theta_{\text{reh}})$ then the data provide us with some non-trivial information on reheating.

In practice, the prior distributions for the θ_{inf} have been chosen exactly as in Ref. [3] while the prior for the cosmological, astrophysical and experimental nuisance parameters are the same as in Ref. [1]. The prior on R_{reh} follows from the requirements that $\rho_{\text{nuc}} < \rho_{\text{reh}} < \rho_{\text{end}}$, where $\rho_{\text{nuc}} \simeq (10 \text{ MeV})^4$ and $-1/3 < \bar{w}_{\text{reh}} < 1$. From Eqs. (2) and (4), this leads to

$$\ln \left(\frac{\rho_{\text{nuc}}^{1/4}}{M_{\text{Pl}}} \right) < \ln R_{\text{reh}} < -\frac{1}{3} \ln \left(\frac{\rho_{\text{nuc}}^{1/4}}{M_{\text{Pl}}} \right) + \frac{4}{3} \ln \left(\frac{\rho_{\text{end}}^{1/4}}{M_{\text{Pl}}} \right). \quad (5)$$

Since the order of magnitude of R_{reh} is a priori unknown, we have chosen a uniform prior on $\ln R_{\text{reh}}$ in the above range. Concerning data analysis, we have used the public likelihood provided by the Planck Collaboration [31]. In order to perform 200 data analyses of the Planck data, one for each \mathcal{M}_i , we have followed the method detailed in Ref. [32]. It requires the evaluation of a marginalized likelihood in the slow-roll parameter space followed by nested sampling analysis for each model \mathcal{M}_i . For this purpose, we have used modified versions of the CAMB [33], COSMOMC [34] and MultiNest [35] codes as well as our public library ASPIC [22].

Let us now turn to the results. In Fig. 1, we have represented the prior-to-posterior standard deviation ratio of $\ln R_{\text{reh}}$, $\Delta\pi_{\ln R_{\text{reh}}}/\Delta\mathcal{P}_{\ln R_{\text{reh}}}$, versus the logarithm of the statistical evidence, $\ln(\mathcal{E}/\mathcal{E}_{\text{best}})$, for all the *Encyclopædia Inflationaris* scenarios. The quantity $\Delta\pi_{\ln R_{\text{reh}}}/\Delta\mathcal{P}_{\ln R_{\text{reh}}}$ measures how much reheating is constrained for a given model. Clearly, if it equals unity (see the dashed horizontal line in Fig. 1), then the posterior is as wide as the prior and there is no information gain. If, on the contrary, $\Delta\pi_{\ln R_{\text{reh}}}/\Delta\mathcal{P}_{\ln R_{\text{reh}}} > 1$, then the posterior is more peaked than the prior and the data carry information on reheating. The quantity $\ln(\mathcal{E}/\mathcal{E}_{\text{best}})$ describes the performance of a model in explaining the data so that models on the right in Fig. 1 are more probable than those on the left. The four vertical dashed lines refer to the four Jeffreys’ categories which measure strength of belief [37]. From right to left, they correspond to models which are inconclusive, weakly disfavored, moderately disfavored and strongly disfavored. In order to quantify

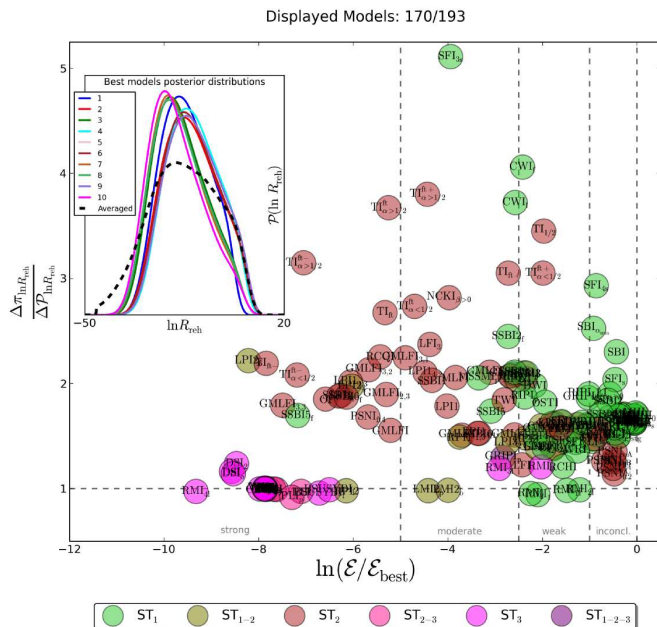


FIG. 1: Prior-to-posterior width ratio of the reheating parameter $\ln R_{\text{reh}}$ versus the logarithm of the Bayesian evidence for the *Encyclopædia Inflationaris* scenarios. Each model is represented by a circle, the color of which refers to the Schwarz-Terrero Escalante classification [36], and an acronym matching the *Encyclopædia Inflationaris* classification [22]. The vertical dashed lines separate the four Jeffreys' categories: inconclusive, weakly disfavored, moderately disfavored and strongly disfavored, from right to left. The dashed horizontal line corresponds to a prior-to-posterior width ratio equal to unity. Models above this line have a reheating stage which is constrained (the higher in the plot the more it is constrained). The inset displays the posterior distributions of $\ln R_{\text{reh}}$ for the ten best Planck 2013 models (KMIII, $\text{ESI}_{\sqrt{2}}$, BI_{6s} , MHI_s , BI_s , ESI , BI_{5s} , KKLTI_s , KMII , BI_{4s}). The thick black dashed line corresponds to the averaged distribution over all *Encyclopædia Inflationaris* models weighted by their Bayesian evidence.

to which extent the reheating stage is constrained, we introduce the following measure

$$\left\langle \frac{\Delta\pi_{\ln R_{\text{reh}}}}{\Delta\mathcal{P}_{\ln R_{\text{reh}}}} \right\rangle \equiv \frac{1}{\sum_j \mathcal{E}_j} \sum_i \mathcal{E}_i \left(\frac{\Delta\pi_{\ln R_{\text{reh}}}}{\Delta\mathcal{P}_{\ln R_{\text{reh}}}} \right)_i, \quad (6)$$

which is the mean value of $\Delta\pi_{\ln R_{\text{reh}}}/\Delta\mathcal{P}_{\ln R_{\text{reh}}}$ weighted by the Bayesian evidence, i.e. the mean value in the space of models. This is a fair estimate since inefficient models will not contribute a lot to this quantity due to their small evidence. Numerically, one obtains $\langle \Delta\pi_{\ln R_{\text{reh}}}/\Delta\mathcal{P}_{\ln R_{\text{reh}}} \rangle \simeq 1.66$ which, therefore, indicates that reheating is indeed constrained by Planck 2013. On average, the posterior distribution of the reheating parameter is 0.60 times smaller than the prior corresponding to a reduction of the prior volume by 40%. This is our main result.

One can also discuss how reheating is constrained

within each of the Jeffreys' categories. We find that the mean value of $\Delta\pi_{\ln R_{\text{reh}}}/\Delta\mathcal{P}_{\ln R_{\text{reh}}}$ is 1.65 for the inconclusive models, 1.63 for the weakly disfavored models, 2.10 for the moderately disfavored models and 1.92 for the strongly disfavored models. The tendency to have stronger constraints for disfavored models is expected. There is indeed relatively small evidence for these scenarios because, in part, some reheating histories are in contradiction with the data and hence are constrained. We also see that the result $\langle \Delta\pi_{\ln R_{\text{reh}}}/\Delta\mathcal{P}_{\ln R_{\text{reh}}} \rangle \simeq 1.66$ is dominated by the inconclusive models precisely because the other models are penalized by their small evidence.

Instead of taking the most generic parametrization, namely $\theta_{\text{reh}} = R_{\text{reh}}$, we have also performed the same analysis using a more restrictive reheating assumption, namely that the mean equation of state parameter \bar{w}_{reh} is known. In that situation, reheating is completely specified by $\theta_{\text{reh}} = \rho_{\text{reh}}$, where $\rho_{\text{reh}}^{1/4}$ measures the reheating temperature. In Fig. 2, we have represented the prior-to-posterior width ratio $\Delta\pi_{\ln \rho_{\text{reh}}}/\Delta\mathcal{P}_{\ln \rho_{\text{reh}}}$ versus the logarithm of the evidence, $\ln(\mathcal{E}/\mathcal{E}_{\text{best}})$ for different equation of state parameters $\bar{w}_{\text{reh}} = -0.3, -0.2, 0$ and 0.2 . One obtains $\langle \Delta\pi_{\ln \rho_{\text{reh}}}/\Delta\mathcal{P}_{\ln \rho_{\text{reh}}} \rangle \simeq 1.55, 1.22, 1.03$, and 1.00 for $\bar{w}_{\text{reh}} = -0.3, -0.2, 0$ and 0.2 , respectively. Such a trend can be seen in Fig. 2 in which the models have a tendency to cluster around the horizontal line $\Delta\pi_{\ln \rho_{\text{reh}}}/\Delta\mathcal{P}_{\ln \rho_{\text{reh}}} = 1$ as \bar{w}_{reh} increases. This means that reheating is relatively well-constrained for $\bar{w}_{\text{reh}} \leq 0$ but not when \bar{w}_{reh} becomes positive and approaches $1/3$. Notice that this is expected as $\bar{w}_{\text{reh}} = 1/3$ corresponds to radiation-like reheating and all observable effects on the CMB disappear. For $1/3 < \bar{w}_{\text{reh}} < 1$, reheating remains unconstrained as for $\bar{w}_{\text{reh}} = 0.6$ we still find $\langle \Delta\pi_{\ln \rho_{\text{reh}}}/\Delta\mathcal{P}_{\ln \rho_{\text{reh}}} \rangle \simeq 1$ (not represented). This is in agreement with the expression of the lever arm in Eq. (2).

Finally, our results show that the Bayesian evidence of a given model differs for different values of \bar{w}_{reh} , i.e., depends on the assumptions made on reheating. For instance, for loop inflation $\text{LI}_{\alpha>0}$, the Bayesian evidence varies from $\ln(\mathcal{E}/\mathcal{E}_{\text{best}}) \simeq -0.41$ (inconclusive zone) for $\bar{w}_{\text{reh}} = -0.3$ to -1.11 (weakly disfavored) for $\bar{w}_{\text{reh}} = -0.2$, -2.59 for $\bar{w}_{\text{reh}} = 0$ (moderately disfavored) and -3.27 for $\bar{w}_{\text{reh}} = 0.2$ (moderately disfavored). This means that in order to estimate the performance of a model, the details of reheating now matter and must be part of the model definition.

In conclusion, we have derived the posterior distributions of the parameters describing the kinematics of the reheating era for nearly 200 inflationary scenarios. We have shown that the Planck 2013 CMB data put non-trivial constraints on the reheating epoch. The precise bounds on the reheating parameter, and on the reheating temperature at fixed equation of state, depend on the model under consideration. Under the most generic parametrization, we have found that the Planck data yield to an average reduction of the reheating prior vol-

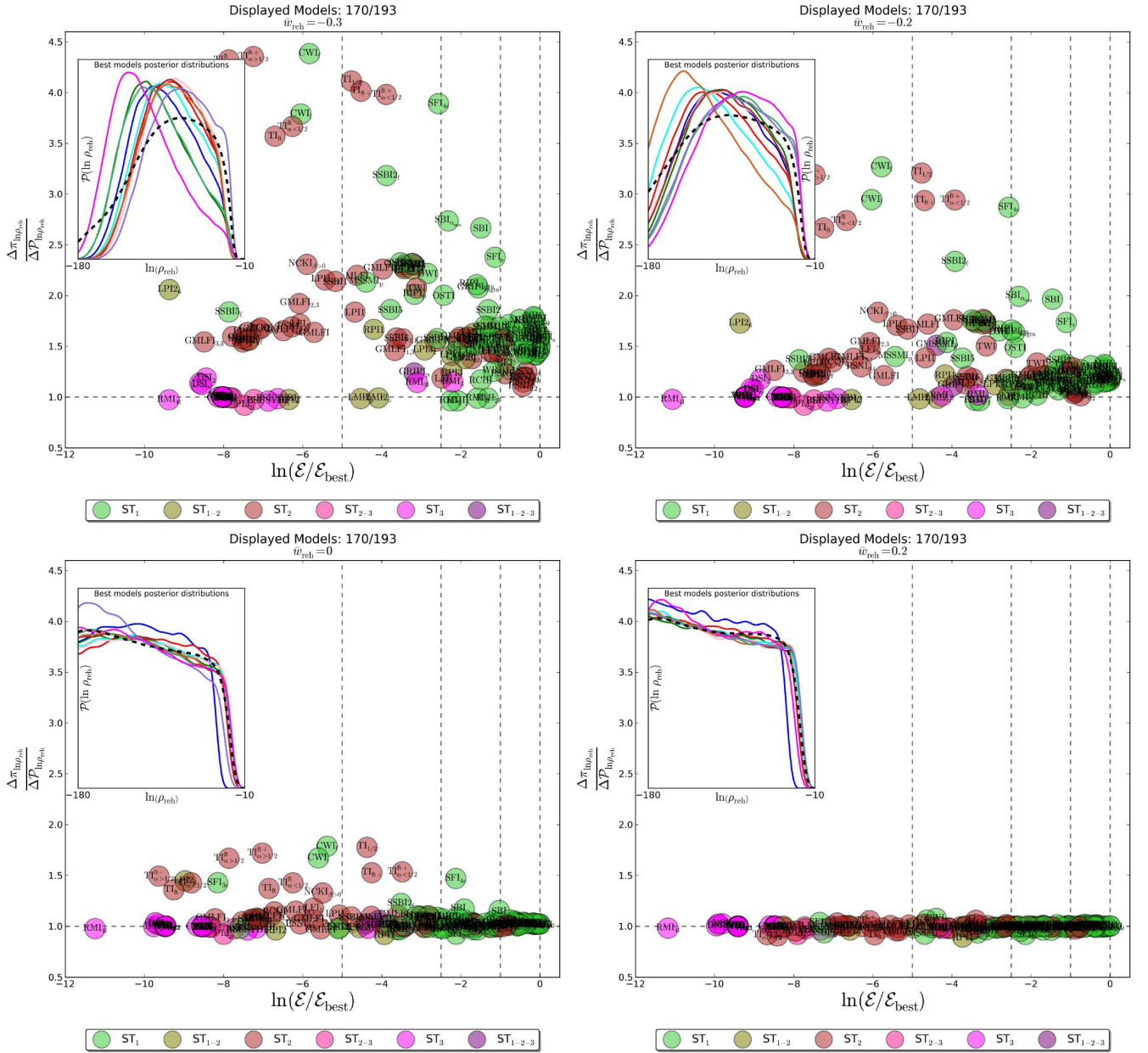


FIG. 2: Same as in Fig. 1 but assuming the mean equation of state during reheating is known. The prior-to-posterior width for the reheating energy density $\ln(\rho_{\text{reh}}/M_{\text{Pl}}^4)$ is represented assuming four values of the mean equation of state \bar{w}_{reh} , namely $\bar{w}_{\text{reh}} = -0.3$ (top left panel), $\bar{w}_{\text{reh}} = -0.2$ (top right panel), $\bar{w}_{\text{reh}} = 0$ (bottom left panel) and $\bar{w}_{\text{reh}} = 0.2$ (bottom right panel). The insets display the posterior distributions of $\ln(\rho_{\text{reh}}/M_{\text{Pl}}^4)$ for the ten best models in each case, namely BI_{3s} , BI_{5s} , BI_{2s} , BI_{4s} , BI_{6s} , KKLT_s , BI_s , RGI_s , $\text{ESI}_{\sqrt{2/3}}$, BI_{1s} for $\bar{w}_{\text{reh}} = -0.3$, BI_{5s} , BI_{4s} , BI_{6s} , BI_{3s} , BI_s , KKLT_s , BI_{2s} , ESI_o , $\text{ESI}_{\sqrt{2/3}}$, $\text{ESI}_{\sqrt{2}}$ for $\bar{w}_{\text{reh}} = -0.2$, KMIII , MHI_s , $\text{ESI}_{\sqrt{2}}$, ESI , $\text{KMII}_{V>0}$, HI , KMII , ESI_o , BI_{6s} , $\text{ESI}_{\sqrt{2/3}}$ for $\bar{w}_{\text{reh}} = 0$ and KMIII , MHI_s , $\text{KMII}_{V>0}$, ESI , $\text{ESI}_{\sqrt{2}}$, KMII , HI , ESI_o , $\text{ESI}_{\sqrt{2/3}}$, BI_{6s} for $\bar{w}_{\text{reh}} = 0.3$.

ume by 40% in the whole space of models tested. In more detail, from the results presented here, we can infer the bounds on $\rho_{\text{reh}}^{1/4}$ for each model of *Encyclopædia Inflationaris*. Because of space limitation, we do not reproduce all of them but it is interesting to give a few examples. For small field scenarios SFI, a case already considered in

Ref. [17], we find, at 95% of confidence, $\rho_{\text{reh}}^{1/4} > 400 \text{ TeV}$ for $\bar{w}_{\text{reh}} = -0.3$, $\rho_{\text{reh}}^{1/4} > 90 \text{ TeV}$ for $\bar{w}_{\text{reh}} = -0.2$, and no constraint for larger values of \bar{w}_{reh} . Better constraints can be found for other models. For supergravity brane inflation SBI, one obtains $\rho_{\text{reh}}^{1/4} > 3.0 \times 10^6 \text{ TeV}$

($w_{\text{reh}} = -0.3$), $\rho_{\text{reh}}^{1/4} > 1.8 \times 10^4 \text{ TeV}$ ($w_{\text{reh}} = -0.2$), and $\rho_{\text{reh}}^{1/4} > 11 \text{ GeV}$ for $w_{\text{reh}} = 0$. For $w_{\text{reh}} = 0.6$, the reheating temperature becomes bounded from above: $\rho_{\text{reh}}^{1/4} < 3.8 \times 10^{11} \text{ TeV}$ (and, hence, reheating cannot be instantaneous in that case). Finally, for $\text{LI}_{\alpha>0}$, one obtains upper bounds on the reheating temperature even for $\bar{w}_{\text{reh}} \leq 0$, namely $\rho_{\text{reh}}^{1/4} < 1.8 \times 10^7 \text{ TeV}$ ($\bar{w}_{\text{reh}} = -0.3$), $\rho_{\text{reh}}^{1/4} < 6.5 \times 10^7 \text{ TeV}$ ($\bar{w}_{\text{reh}} = -0.2$), $\rho_{\text{reh}}^{1/4} < 4.0 \times 10^{10} \text{ TeV}$ ($\bar{w}_{\text{reh}} = 0$), and $\rho_{\text{reh}}^{1/4} < 5.1 \times 10^{11} \text{ TeV}$ for $\bar{w}_{\text{reh}} = 0.2$.

Another result found in this Letter is that the Bayesian evidence of a model can change in a non negligible way according to the assumptions made on its reheating properties. This indicates that, with high accuracy CMB data, reheating details are now important. Obviously, this will become even more relevant in the case of future CMB missions [38]. The results presented here represent the first complete survey of what can be deduced about inflationary reheating from the Planck data.

The work of C. R. is supported by the ESA Belgian Federal PRODEX Grant No. 4000103071 and Wallonia-Brussels Federation Grant ARC No. 11/15-040. The work of V. V. is supported by STFC grant ST/L005573/1.

* Electronic address: jmartin@iap.fr

† Electronic address: christophe.ringeval@uclouvain.be

‡ Electronic address: vincent.vennin@port.ac.uk

- [1] P. Ade et al. (Planck Collaboration), *Astron.Astrophys.* **571**, A16 (2014), 1303.5076.
- [2] P. Ade et al. (Planck Collaboration), *Astron.Astrophys.* **571**, A22 (2014), 1303.5082.
- [3] J. Martin, C. Ringeval, R. Trotta, and V. Vennin, *JCAP* **1403**, 039 (2014), 1312.3529.
- [4] M. S. Turner, *Phys. Rev.* **D28**, 1243 (1983).
- [5] J. H. Traschen and R. H. Brandenberger, *Phys.Rev.* **D42**, 2491 (1990).
- [6] L. Kofman, A. D. Linde, and A. A. Starobinsky, *Phys. Rev.* **D56**, 3258 (1997), hep-ph/9704452.
- [7] B. A. Bassett, S. Tsujikawa, and D. Wands, *Rev.Mod.Phys.* **78**, 537 (2006), astro-ph/0507632.
- [8] J. Braden, L. Kofman, and N. Barnaby, *JCAP* **1007**, 016 (2010), 1005.2196.
- [9] A. V. Frolov, *Class.Quant.Grav.* **27**, 124006 (2010), 1004.3559.
- [10] R. Allahverdi, R. Brandenberger, F.-Y. Cyr-Racine, and A. Mazumdar, *Ann.Rev.Nucl.Part.Sci.* **60**, 27 (2010), 1001.2600.
- [11] M. Drewes and J. U. Kang, *Nucl.Phys.* **B875**, 315 (2013), 1305.0267.
- [12] M. A. Amin, M. P. Hertzberg, D. I. Kaiser, and J. Karouby, *Int.J.Mod.Phys.* **D24**, 1530003 (2015), 1410.3808.
- [13] M. P. Hertzberg, J. Karouby, W. G. Spitzer, J. C. Bécerra, and L. Li, *Phys.Rev.* **D90**, 123528 (2014), 1408.1396.
- [14] J. Martin and C. Ringeval, *JCAP* **0608**, 009 (2006), astro-ph/0605367.
- [15] L. Lorenz, J. Martin, and C. Ringeval, *JCAP* **0804**, 001 (2008), 0709.3758.
- [16] C. Ringeval, *Lect. Notes Phys.* **738**, 243 (2008), astro-ph/0703486.
- [17] J. Martin and C. Ringeval, *Phys.Rev.* **D82**, 023511 (2010), 1004.5525.
- [18] V. Demozzi and C. Ringeval, *JCAP* **1205**, 009 (2012), 1202.3022.
- [19] C. Ringeval, T. Suyama, and J. Yokoyama, *JCAP* **1309**, 020 (2013), 1302.6013.
- [20] R. Easther and H. V. Peiris, *Phys.Rev.* **D85**, 103533 (2012), 1112.0326.
- [21] L. Dai, M. Kamionkowski, and J. Wang, *Phys.Rev.Lett.* **113**, 041302 (2014), 1404.6704.
- [22] J. Martin, C. Ringeval, and V. Vennin, *Phys.Dark Univ.* (2014), 1303.3787, URL <http://cp3.irmp.ucl.ac.be/~ringeval/aspic.html>.
- [23] T. Giannantonio and E. Komatsu, *Phys.Rev.* **D91**, 023506 (2015), 1407.4291.
- [24] D. Spergel et al. (WMAP Collaboration), *Astrophys.J.Suppl.* **170**, 377 (2007), astro-ph/0603449.
- [25] N. Jarosik, C. Bennett, J. Dunkley, B. Gold, M. Greason, et al., *Astrophys.J.Suppl.* **192**, 14 (2011), 1001.4744.
- [26] J. Martin, C. Ringeval, and R. Trotta, *Phys.Rev.* **D83**, 063524 (2011), 1009.4157.
- [27] S. Kuroyanagi, C. Ringeval, and T. Takahashi, *Phys.Rev.* **D87**, 083502 (2013), 1301.1778.
- [28] S. Kuroyanagi, K. Nakayama, and J. Yokoyama (2014), 1410.6618.
- [29] R. Trotta, *Mon.Not.Roy.Astron.Soc.* **378**, 72 (2007), astro-ph/0504022.
- [30] R. Trotta, *Contemp.Phys.* **49**, 71 (2008), 0803.4089.
- [31] P. Ade et al. (Planck Collaboration), *Astron.Astrophys.* **571**, A15 (2014), 1303.5075.
- [32] C. Ringeval, *Mon. Not. Roy. Astron. Soc.* **439**, 3253 (2014), 1312.2347.
- [33] A. Lewis, A. Challinor, and A. Lasenby, *Astrophys.J.* **538**, 473 (2000), astro-ph/9911177.
- [34] A. Lewis and S. Bridle, *Phys.Rev.* **D66**, 103511 (2002), astro-ph/0205436.
- [35] F. Feroz, M. Hobson, and M. Bridges, *Mon.Not.Roy.Astron.Soc.* **398**, 1601 (2009), 0809.3437.
- [36] D. J. Schwarz, C. A. Terrero-Escalante, and A. A. Garcia, *Phys.Lett.* **B517**, 243 (2001), astro-ph/0106020.
- [37] C. Gordon and R. Trotta, *Mon.Not.Roy.Astron.Soc.* **382**, 1859 (2007), 0706.3014.
- [38] J. Martin, C. Ringeval, and V. Vennin, *JCAP* **1410**, 038 (2014), 1407.4034.